CHAPTER 3

COALESCENCE AND BREAKUP

In this chapter, rate models for turbulent bubble coalescence and breakup, as well as the daughter bubble size distribution for breakage, are developed based on the principles of molecular collision, isotropic turbulence and probability. Unlike previous work, this coalescence rate model has only one unknown constant and shows that the coalescence rate as a function of bubble size may appear a clear maximum.

The theoretical bubble breakage rate model has no adjustable parameters and all the constants in the model are calculated from the constants of isotropic turbulence theory. The breakage daughter bubble size distributions can be derived directly from the breakage rate model and show very good agreement with the experimental results of Hesketh *et al.* (1991a).

The developed rate models may also be applied to turbulent liquid-liquid dispersions.

3.1 Introduction

Turbulent gas-liquid dispersed flow not only is of the most basic characteristics of bubble column reactors, but is also often encountered in many other industrial devices such as sieve plate columns for distillation or gas purification and floatation tanks for ore-concentration. In most of these devices, the main purpose of the gas dispersion is to achieve large gas-liquid interfacial areas and thereby to obtain rapid mass transfer. The gas dispersion also greatly enhances heat transfer rates to solid surfaces and is thus also important for highly exothermic reaction processes. The rate of interfacial transport of mass and heat is often a key design criterion and may limit productivity and control reaction selectivity. Much of the uncertainty related to the transfer rates is buried in the lack of confident information on the bubble size distributions and the gas-liquid interfacial structure. In current design of bubble columns, the information is mainly determined by direct experimentation or based on empirical correlations.

Bubble coalescence and breakup are basic processes taking place, and are specific characteristics of a given gas-liquid dispersion. They are increasingly considered as important processes, because they not only govern the bubble size distribution but also directly affect interfacial mass transfer by the renewal of bubble surfaces. For example, a balance, or an equilibrium, between rates of coalescence and breakup may be considered to control the bubble size distribution in a bubble column system, as done by Prince and Blanch (1990). The modeling of bubble coalescence and breakup rates is very complex and is based on the knowledge of collision or breakup frequencies, breakage daughter bubble size distributions and probabilities of coalescence and breakup. At present the understanding of these underlying processes is still insufficient.

Some effort has been directed at establishing coalescence and breakup models for fluid particles in dispersions. However, most of the work has been concerned with liquid drops in stirred tank systems. Some of the early work aimed at establishing methods for estimation of stable bubble or drop sizes. For example, Hinze (1955) made a semi-quantitative analysis on the forces controlling deformation and breakup of fluid particles and developed methods to estimate a stable bubble or drop size in a dispersion system relying on two dimensionless groups: a Weber group and a viscosity group. Hughmark (1971) proposed a semi-empirical correlation to predict the stable drop size in turbulent pipe flow based on the work of Hinze (1955).

The analysis and modeling of the coalescence and breakup rate processes has been paid greater attention. Valentas and Amundson (1966) gave a detailed analysis of the processes of drop coalescence and breakup in stirred tanks. For the coalescence processes, they proposed the concepts of collision frequency and coalescence efficiency, the latter assumed to be a function of the difference between the individual drop sizes and the stable drop size. For the breakup processes, a breakup model was proposed where the rate was assumed to be inversely proportional to the characteristic breakage time, a tuning parameter. At the same time, combined with a mean number of drops formed per breakage, a daughter droplet size distribution, or breakage kernel, was proposed and was assumed to be a delta function or a normal density function (Valentas *et al.*, 1966). This concept was utilized by some of the later investigators. Mihail and Straja (1986) also proposed both coalescence and breakage efficiency models for bubbles in bubble columns, analogous to the work of Valentas and Amundson (1966). They introduced the collision and breakup efficiencies as functions of the difference between the individual bubble sizes and a maximum size using four tuning parameters.

Some work has been done to obtain efficiencies or rates of coalescence and breakup through more fundamental analyses instead of by direct assumptions. Kuboi *et al.* (1972b) used an empirical correlation including a "modified kinetic energy" as a variable for estimating the coalescence probability for binary equal sized drop collisions in turbulent liquid flows.

Coulaloglou and Tavlarides (1977) assumed identical kinetic energy distributions for drops and turbulent eddies in order to develop drop breakup efficiencies. They also assumed the motion of daughter drops to be similar to that of turbulent eddies and could thereby estimate the "characteristic breakup time". Based on this, for stirred tanks, a drop breakup model with two unknown parameters was proposed. The breakage daughter drop size distribution was by the authors assumed to follow a normal density function. In addition, they proposed a phenomenological model with two unknown parameters for binary drop coalescence using the dimensional analysis developed by Levich (1962) to estimate the interaction time between two colliding drops, together with the relationship given by Chappelear (1963) for estimating the coalescence time of drops.

Chatzi *et al.* (1989) proposed drop coalescence and breakup models based on, and very similar to, the models of Coulaloglou and Tavlarides (1977). Prince and Blanch (1990) also followed the same procedure as Coulaloglou and Tavlarides (1977) in order to develop efficiency models for bubble coalescence and breakage. They used a different energy distribution function in the breakage efficiency model and a different coalescence time relationship in the coalescence efficiency model.

Narsimhan *et al.* (1979) have given a more theoretical analysis, based on probability theory, and have proposed a binary drop breakage model based on such assumptions as the number of eddies arriving on the surface of a droplet being a Poisson process, the arrival frequency of eddies being constant and a uniform daughter droplet size distribution. Lee *et al.* (1987a) also proposed bubble coalescence and breakage models. The bubble breakage model was developed based on the work of Narsimhan *et al.* (1979) and used the similar assumptions. In their coalescence model, the interaction time correlation proposed by Levich (1962) according to dimensionless analysis was used.

Recently, Nambiar *et al.* (1992) have developed a drop breakage model for stirred tanks based on the interaction between a drop and the eddies of length scales smaller than the drop diameter. They have concluded daughter drop size distributions completely contradicting the normal or uniform density functions usually assumed.

Many of the models mentioned above are inconsistent with each other and have two or more unknown parameters. This is mainly due to the general lack of information making it necessary to resort to many assumptions, some of which even contradicting experimental evidence. For example, the breakage daughter bubble or drop size distribution has usually been assumed to be a delta or normal function, having the highest probability for the equal-sized breakage. However, recent experimental work of Hesketh *et al.* (1991a) has shown that the equal-sized breakage in turbulent flow has the lowest probability. The daughter bubble or drop size distributions will be discussed in detail later in this chapter.

The work in this chapter is aimed at developing fundamental rate models for the bubble coalescence and breakage processes in turbulent gas-liquid dispersion systems such as bubble columns.

3.2 Binary Bubble Coalescence

It is usually considered that coalescence of two bubbles in liquids occurs in three steps. First, the bubbles collide, trapping a small amount of liquid between them. This liquid then drains out until the liquid film separating the bubbles reaches a critical thickness, at which film rupture occurs, resulting in coalescence. Since two bubbles must collide and then keep in contact for a sufficient time for coalescence to occur through the processes of film drainage and rupture, the coalescence process can be analyzed by examining the collision events and the efficiency (probability) of a collision resulting in coalescence. In other words, the rate of bubble coalescence will depend on the collision frequency and the fraction of collisions resulting in coalescence (the so-called coalescence efficiency or coalescence probability). Thus, for the coalescence between bubble i and bubble j with sizes v_i or d_i and v_j or d_j respectively the coalescence rate can be expressed by

$$\Omega_C(v_i:v_j) = \omega_C(v_i:v_j)P_C(v_i:v_j) \tag{3.1}$$

where ω_C and P_C are the collision frequency and the coalescence efficiency of bubbles respectively. The collision frequency is a complex function of the bubble or drop number densities, the size distributions and of the flow structure of the continuous phase. For example, an increase in the approach velocities can increase collision frequency and thereby increase the coalescence rate. However, it can also supply the two bubbles with sufficient energy to cause a rebound before coalescence can occur, resulting in a lower coalescence efficiency and thereby decreasing the overall coalescence rate. The coalescence efficiency depends on the forces acting on the colliding bubbles during the approach process since the interaction time between two bubbles is tied to these forces (Chapter 4; Chesters, 1991; Jeelani and Hartland, 1991).

Bubble coalescence in gas-liquid dispersions has been considered to take place due to a variety of mechanisms such as turbulence, shear stress and buoyancy (Friedlander, 1977; Prince and Blanch, 1990). However, regardless of mechanism, collision is the first step and a necessary condition for coalescence to occur. In addition, since the collision of three or more bubbles at the same time has a very small probability, only binary collisions or binary coalescence is usually considered. This is also done in the present work.

3.2.1 Binary bubble collision frequency

Turbulent collisions result from the more or less random motion of bubbles due to turbulence in a dispersed two-phase system. However, due to the complexity of turbulence, to determine the mean relative velocity between bubbles involved in turbulent collisions, some simplifications have to be made.

Firstly, to make the problem tractable, the turbulence is usually assumed to be isotropic (*e.g.* Lee *et al.* 1987a; Prince and Blanch, 1990). Although the turbulence in bubble columns is usually non-isotropic as shown by Menzel (1990), the isotropic turbulence assumption is also used by this work. This is because theoretical considerations and experimental evidence has shown, as concluded by Hinze (1959), that the fine-scale structure of most actual non-isotropic turbulent flows is locally nearly isotropic. Many features of isotropic turbulence may thus apply to phenomena in actual turbulence that are determined mainly by the fine-scale structure (Hinze, 1959). Furthermore, even an actual turbulence situation with a non-isotropic large-scale structure or which is non-isotropic through an essential part of its spectrum, can often as a first approximation be treated as if it were isotropic. The differences between results based upon the assumed isotropy and actual results are often sufficiently small to be disregarded compared to the uncertainty of the experimental data (Hinze, 1959).

Another assumption used in this work is that the bubble sizes lie in the inertial subrange of isotropic turbulence, as also done by the authors mentioned above. The criteria for the inertial subrange are

$$k_e < k < k_d \quad or \quad \lambda_e > \lambda > \lambda_d \tag{3.2}$$

where k_e and λ_e are the wave number and the size of the large energy containing eddies respectively, and k_d and λ_d are those eddies where the viscous dissipation takes place. Since $\lambda_d = (\nu_L^3/\varepsilon)^{1/4}$ or $k_d = (\varepsilon/\nu_L^3)^{1/4}$ and λ_e is of the same order as the scale of equipment, the bubble sizes can usually satisfy these criteria in practice, that is, be much larger than the micro scale of turbulence and much less than the diameter of the equipment. Hence, this assumption may be reasonable.

In order to determine the mean approach velocity of bubbles in turbulent collisions, it is assumed that the colliding bubbles take the velocity of the turbulent eddies having the same size as the bubbles (*e.g.* Coulaloglou and Tavlarides, 1977; Lee *et al.* 1987a; Prince and Blanch, 1990). Considering that a small eddy does not contain sufficient energy to affect bubble motion and that an eddy much larger than the bubble nearly has no effect on the relative motion of bubbles, this assumption may also be acceptable.

The mean turbulent velocity of eddies with size λ in the inertial subrange of isotropic turbulence can be expressed by (Kuboi, *et al.*, 1972a,b):

$$\bar{u}_t = \left(\frac{8\overline{u^2}}{3\pi}\right)^{1/2} = \left(\frac{8\beta}{3\pi}\right)^{1/2}(\varepsilon\lambda)^{1/3} = \beta^{1/2}(\varepsilon\lambda)^{1/3} \tag{3.3}$$

where the constant, $\beta = (3/5)\Gamma(1/3)\alpha$ (here α is a universal constant in turbulence theory), as given by Batchelor (1953) using turbulence theory, is about 2.41 as $\alpha = 1.5$ (Tennekes and Lumley, 1972). The measured value of β is 2.0 according to Kuboi *et al.* (1972a). When the above equation is used to determine bubble velocities, the eddy size, λ, is substituted by the bubble diameter.

Assuming that the bubble velocities due to the turbulent eddies are statistically non-correlated in space, analogous to the motion of ideal gas molecules, the mean approach velocities of the bubbles in turbulent collisions can be determined by the mean square root of the bubble velocities (Kuboi *et al.*, 1972b; Lee *et al.*, 1987a; Prince and Blanch, 1990), that is

$$\bar{u}_{ij} = \left(\bar{u}_i^{\,2} + \bar{u}_j^{\,2}\right)^{1/2} = \bar{u}_i\left(1 + \xi_{ij}^{-2/3}\right)^{1/2} \tag{3.4}$$

where the size ratio, $\xi_{ij} = d_i/d_j$ and $\bar{u}_i$ or $\bar{u}_j$ is the bubble velocity calculated by Equation (3.3) substituting d_i or d_j for λ.

Knowing the approach velocity for the turbulent collisions, the collision frequency can be calculated using an expression developed by Saffman and Turner (1956) for binary drop collisions in turbulent air, analogous to that for collisions of gas molecules:

$$\omega_C = \frac{\pi}{4}(d_i + d_j)^2 n_i n_j \bar{u}_{ij} \tag{3.5}$$

This expression for the collision frequency of bubbles or drops has been verified by Kuboi *et al.* (1972b) using the experimental results for the collisions of equal-sized drops in benzene-water and cyclohexanone-water systems and has been used by authors such as Lee *et al.* (1987a) and Prince and Blanch (1990).

3.2.2 Coalescence efficiency

Up to now, coalescence efficiency models are mainly based on the phenomenological analyses. According to coalescence theory (Ross *et al.*, 1978; Chesters, 1991), coalescence will occur for a collision of two bubbles provided that the contact time (interaction time), t_I, exceeds the coalescence time, t_C, required for drainage of the liquid film between them to a critical rupture thickness. The ratio t_C/t_I can thus provide a first indication of whether coalescence will or will not occur under given conditions, that is, a coalescence efficiency (coalescence probability) going to zero for large values of this ratio and to unity for small ones can be defined. A simple function satisfying these characteristics is

$$P_C = \exp\left(-\frac{t_C}{t_I}\right) \tag{3.6}$$

This concept has been used by many authors (*e.g.* Coulaloglou and Tavlarides, 1977; Ross, *et al.*, 1978; Lee, *et al.*, 1987; Prince and Blanch, 1990; Chesters, 1991), but the various authors have used different interaction and coalescence times. Obviously, this is an empirical relationship in reality. Nevertheless, it may be a better approximation when more fundamental knowledge on the coalescence efficiency is in the lack. Therefore, it is still used in this work.

Once Equation (3.6) is acceptable, the predominant problem becomes how to obtain the correct interaction and coalescence times. These times are dependent on the collision forces and the approach velocities. In addition, the surface properties of the bubbles are also important and significantly affect the coalescence time. Hence, the coalescence efficiency will be a function of the relative importance of the various coalescence mechanisms and of the surface situation. In practical gas-liquid dispersions, collisions or coalescence is usually between equal or unequal-sized bubbles with deformable and partially mobile interfaces. Unfortunately, most of the research work on the coalescence time available from the literature is for the equal sized bubbles or drops with fully mobile interfaces. However, a coalescence time expression developed by Chesters (1991) for the coalescence between deformable and fully mobile interfaces due to turbulence in the inertial subrange has been considered to be also suitable for the unequal sized cases. Hence, although many cases encountered in practice are partial-fully mobile interfaces, this expression is still used in this work. It can be written as

$$t_C = 0.5\frac{\rho_L \bar{u}_{ij} d_i^2}{(1+\xi_{ij})^2 \sigma} \tag{3.7}$$

For the interaction time in turbulent systems, most of the previous studies used the relationship developed by Levich (1962) based on dimensional analysis. An equation for the interaction time was proposed by Chesters (1991), but it is only suitable for equal sized fluid particles. In order to find a more reasonable and fundamental expression for the interaction time of two equal and unequal sized fluid particles, a bubble or drop approach model has been developed in Chapter 4, based on the parallel film concept. This model gives an equation for determining the interaction time as follows,

$$t_I = 2t_{\max} = (1+\xi_{ij})\sqrt{\frac{(\rho_G/\rho_L+\gamma)}{3(1+\xi_{ij}^2)(1+\xi_{ij}^3)}\frac{\rho_L d_i^3}{\sigma}} \tag{3.8}$$

where t_{max} is the time between the first contact and when the film area between the two colliding bubbles reaches its maximum value (see Chapter 4).

Substituting Equations (3.7) and (3.8) into Equation (3.6), the coalescence efficiency can be obtained as follows

$$P_C = \exp\left\{-c_1\frac{[0.75(1+\xi_{ij}^2)(1+\xi_{ij}^3)]^{1/2}}{(\rho_G/\rho_L+\gamma)^{1/2}(1+\xi_{ij})^3}We_{ij}^{1/2}\right\} \tag{3.9}$$

Here c_1 is a unknown constant of order unity and has to be adjusted. The Weber number, We_{ij} is defined by

$$We_{ij} = \frac{\rho_L d_i \bar{u}_{ij}^2}{\sigma} \tag{3.10}$$

Equation (3.9) gives the coalescence efficiency is a function of the Weber number, the bubble size ratio, the virtual mass coefficient and the physical properties of the system.

Now, the coalescence rate can be calculated by Equations (3.1), (3.9) and (3.5), if the bubble number densities are known.

3.3 Model for Bubble Breakup

As mentioned before, the bubbles in a turbulent dispersion are not only exposed to a turbulent field, but will also be subject to both inertial and viscous forces. However, when concerned with bubble breakage, the viscous forces can usually be neglected since the bubbles are much larger than the microscale of turbulence (Shinnar, 1961; Narsimhan *et al.*, 1979). In such a case, a bubble of sufficient size will oscillate around its spherical equilibrium. The oscillations are brought about by the kinetic energy of the turbulent motion in the continuous phase or, by the relative velocity fluctuations between points near the vicinity of the bubble surface. In other words, the kinetic energy of the turbulent motion brings about an increase in the surface energy of the bubble through deformations. Fragmentation of the bubble occurs if the turbulent motion provides an increase in surface energy sufficient to cause breakage.

In a turbulent field, velocity fluctuations at a point can be thought of as due to the arrival of eddies of different scales (frequencies). Similarly, the relative velocity fluctuations around the surface of a bubble exposed to a turbulent field can be viewed as caused by the arrival of eddies with different scales and frequencies at the surface of the bubble. This is equivalent to the "bombarding" of eddies on the bubble surface.

Analogous to droplets in turbulence (Narsimhan *et al.*, 1979), oscillations of a bubble induced by a particular eddy may be interrupted by the arrival of subsequent eddies. Whether or not this occurs, is governed by the relative magnitudes of the time scales of, (i) the eddy arrival process and (ii) the oscillations of the bubble. If the two time scales are comparable the effects of successive eddies continually interfere with each other. Since oscillations of a bubble, that may make the bubble break, are caused only by the hitting of eddies with the scale similar or smaller than the bubble diameter, the smaller bubbles require very small eddies to induce the oscillations. Furthermore, the time scale of oscillations should be inversely proportional to the eddy frequency. Thus the smaller eddies may be expected to create high frequency oscillations.

In what follows, the assumption, which was also used by Narsimhan *et al.* (1979) and Lee *et al.* (1987a), is employed. This is that the time scale of the oscillation is smaller than that associated with eddy arrival, so that once an eddy of sufficiently high energy arrives, the bubble will certainly break.

3.3.1 Arrival or bombarding frequency of eddies

The arrival frequency of eddies with a special size λ on the surface of bubbles with size d_i is equivalent to the collision frequency between the eddies and the bubbles (or the bombarding frequency of the eddies on the bubbles). The collision frequency of eddies of a size between λ and $\lambda+d\lambda$ on bubbles of size d_i can be expressed by

$$\dot{\omega}_{B,\lambda} = \frac{\pi}{4}(d_i+\lambda)^2\bar{u}_\lambda n_i \dot{n}_\lambda \qquad (3.11)$$

where $\dot{n}_\lambda$ is the number of eddies per unit reactor volume of size between λ and $\lambda+d\lambda$ and $\bar{u}_\lambda$ is the turbulent velocity of eddies of a size λ, given by Equation (3.3), for the eddies in the inertial subrange.

The energy spectrum, $E(k)$, indicates the kinetic energy of eddies of wave number between k and $k+dk$ or size between λ and $\lambda+d\lambda$ per unit mass (Tennekes and Lumley, 1972). When this is known, a relationship between $\dot{n}_\lambda$ and $E(k)$ can be obtained as follows

$$\dot{n}_\lambda \rho_L \frac{\pi}{6}\lambda^3 \frac{\bar{u}_\lambda^2}{2} d\lambda = E(k)\rho_L(1-\varepsilon_G)(-dk) \qquad (3.12)$$

where ε_G is the local gas fraction.

The functional form of the energy spectrum for the whole range of isotropic turbulence is not available, but in the inertial subrange it is well described (Tennekes and Lumley, 1972) by

$$E(k) = \alpha \varepsilon^{2/3} k^{-5/3} \tag{3.13}$$

The relationship between the wave number and the size of an eddy is $k=2\pi/\lambda$ (Tennekes and Lumley, 1972). Therefore, the number of eddies of sizes between λ and $\lambda+d\lambda$ per unit reactor volume, or the number density of eddies, is

$$\dot{n}_{\lambda} = \frac{c_2(1-\varepsilon_G)}{\lambda^4} \tag{3.14}$$

where

$$c_2 = \frac{9\alpha}{2(2\pi)^{2/3}\beta} = \frac{15}{2(2\pi)^{2/3}\Gamma(1/3)} = 0.822 \tag{3.15}$$

Equation (3.14) indicates that smaller eddies have higher number densities. However, the equation is only valid for eddies in the inertial subrange of isotropic turbulence because the used turbulent energy spectrum function and the turbulent velocity are only valid in this subrange. This limitation will probably have an insignificant effect on the eddy bombarding consideration, since the very small eddies have very low energy contents and very short lifetimes.

Consequently, the bombarding frequency for the eddies with size between λ and $\lambda+d\lambda$ on bubbles of size d_i can be expressed as

$$\dot{\omega}_{B,\lambda} = \dot{\omega}_{B,\xi} = c_3(1-\varepsilon_G)n_i(\varepsilon d_i)^{1/3}\frac{(1+\xi)^2}{d_i^2\xi^{11/3}} \tag{3.16}$$

where that $\xi = \lambda/d_i$ is the size ratio between an eddy and the bubble, and

$$c_3 = c_2\pi\beta^{1/2}/4 = 0.923 \tag{3.17}$$

3.3.2 Breakage probability (efficiency)

For a particular eddy hitting a bubble, the likelihood of bubble breakage depends not only on the energy contained in the arriving eddy, but also on the minimum energy requirement by the surface area increase due to bubble fragmentation. The latter is determined by the number and the sizes of the daughter bubbles formed in the breakage processes.

In a breakage, a bubble may break into two or more bubbles with equal or unequal volumes, depending on the breakage type. It is common opinion that there exist two types of breakage for drops or bubbles in turbulent pipeline flow. These are turbulent (deformation) breakage and viscous shear (tearing) breakage (Sleicher, 1962; Collins and Knudson, 1970; Walter and Blanch, 1986 and Hesketh *et al.*, 1991a,b). In the former, the breakage is caused by fluctuating eddies bombarding the bubble surface (Walter and Blanch, 1986) causing oscillations (or deformations) of the bubble surface. Usually, binary breakage occurs in this case. For the latter type, bubbles may break into several bubbles with varying volumes due to viscous shear. Since viscous forces have already been assumed to be of little importance in turbulent dispersions, as discussed before, only the binary breakage is considered to be significant. This consideration is reasonable according to the recent experimental results of Hesketh *et al.* (1991a). They found that all bubble and drop breakage events were binary in turbulent pipeline flows.

For binary breakage, a dimensionless variable describing the sizes of daughter bubbles, the breakage volume fraction, is defined as

$$f_{BV} = \frac{v_I}{v_i} = \frac{d_I^3}{d_i^3} = \frac{d_I^3}{d_I^3 + d_{II}^3} \tag{3.18}$$

where d_I and d_{II} are the diameters (corresponding to volumes v_I and v_{II}) of the daughter bubbles in the binary breakage of a parent bubble with diameter d_i. The value interval for the breakage volume fraction should be $0 < f_{BV} < 1$ ($f_{BV} = 0.5$

means an equal binary breakage and f_{BV} = 0 or 1 means no breakage). Hesketh *et al.* (1991a) found that the value range of f_{BV} was independent of the size of parent bubble. For instance, large bubbles of diameter 6 mm were observed to break into bubbles with f_{BV} values of 0.1 and 0.9, and 0.5 and 0.5. The same values of f_{BV} were also obtained for a small bubble of 2.5 mm. Thus, it is reasonable to assume that the variation range of f_{BV} is independent of the original bubble size.

To determine the energy contained in eddies of different scales, a distribution function of the kinetic energy for eddies in turbulence is required. Lee *et al.* (1987a) used the Maxwell's law for this function. However the Maxwell's law is especially for free gas molecular motion and may not be suitable for turbulent eddies. Angelidou *et al.* (1979) have developed an energy distribution density function for fluid particles in liquids, which satisfies a natural exponential function. Actually, for the kinetic energy of turbulent eddies, this exponential energy density function is found to be equivalent to the common assumption that the velocity distribution of turbulent eddies is a normal density function (Saffman and Turner, 1956; Coulaloglou and Tavlarides, 1977; Narsimhan *et al.*, 1979). This assumption of a normal velocity distribution is also supported by the experimental results of Kuboi *et al.* (1972) for a turbulent liquid-liquid dispersion system. Hence, this distribution function is also used in the present work to describe the kinetic energy distribution of the eddies in turbulence, that is

$$p_e(\chi) = \frac{1}{\bar{e}(\lambda)}\exp(-\chi)\,, \quad \chi = \frac{e(\lambda)}{\bar{e}(\lambda)} \tag{3.19}$$

where the mean kinetic energy of an eddy with size λ, $\bar{e}(\lambda)$, is given by

$$\bar{e}(\lambda) = \rho_L \frac{\pi}{6}\lambda^3 \frac{\overline{u_\lambda^2}}{2} = \frac{\pi\beta}{12}\rho_L(\varepsilon d_i)^{2/3} d_i^3 \xi^{11/3} \tag{3.20}$$

When a bubble of size d_i breaks into two bubbles with a given value of f_{BV}, the increase in surface energy is

$$\overline{e}_i(d_i) = \left[f_{BV}^{2/3} + \left(1 - f_{BV}\right)^{2/3} - 1\right]\pi d_i^2 \sigma = c_f \pi d_i^2 \sigma \tag{3.21}$$

where c_f is defined as the surface area change coefficient that is

$$c_f = f_{BV}^{2/3} + \left(1 - f_{BV}\right)^{2/3} - 1 \tag{3.22}$$

As seen, c_f depends only on the breakage volume fraction, f_{BV}, and is a function symmetrical about $f_{BV} = 0.5$.

Since the time scale of bubble oscillation is assumed to be smaller than that associated with the eddy bombardment, such that once an eddy of sufficiently high energy arrives this leads to certain bubble breakage, then the condition for an oscillating deformed bubble to break is that the kinetic energy of the bombarding eddy exceeds the increase in surface energy required for breakage:

$$e(\lambda) \geq \overline{e}_i(d_i) = c_f \pi d_i^2 \sigma \tag{3.23}$$

Consequently, according to probability theory, the probability for a bubble of size v_i or d_i to break into a size of $v_f = v_i f_{BV}$ when the bubble is hit by an arriving eddy of size λ, will be equal to the probability of the arriving eddy of size λ having a kinetic energy greater than or equal to the minimum energy required for creating the bubble breakup. This gives

$$\begin{aligned} P_B(v_i : v_i f_{BV}, \lambda) &= P_e[e(\lambda) \geq \overline{e}_i(d_i)] = P_e[\chi \geq \chi_c] \\ &= 1 - P_e[\chi \leq \chi_c] \end{aligned} \tag{3.24}$$

where the dimensionless critical breakup energy, χ_c, is given by

$$\chi_c = \frac{\overline{e}_i(d_i)}{\overline{e}(\lambda)} = \frac{12 c_f}{We_i} \xi^{-11/3} \tag{3.25}$$

where

$$We_i = \frac{\rho_L d_i \bar{u}_i^2}{\sigma} \tag{3.26}$$

Then the conditional breakage probability, $P_B(v_i{:}v_if_{BV},\lambda)$, can be expressed as

$$P_B(v_i{:}v_if_{BV},\lambda) = 1 - \int_0^{\chi_c} \exp(-\chi)\,d\chi = \exp(-\chi_c) \tag{3.27}$$

3.3.3 The expression for breakage rate

Since only eddies with size smaller than or equal to the size of a bubble can cause the bubble to oscillate, the breakage rate for bubbles of size v_i forming bubbles of size $v_j = v_if_{BV}$ can be expressed as

$$\Omega_B(v_i{:}v_if_{BV}) = \int_{\lambda_{min}}^{d_i} P_B(v_i{:}v_if_{BV},\lambda)\,\omega_{B,\lambda}\,d\lambda \tag{3.28}$$

The lower limit in the above integral should actually have been the microscale of eddies, λ_d, but it has been replaced by the minimum size of eddies in the inertial subrange of isotropic turbulence, λ_{min}. The reason is that the expressions for bombarding frequency of eddies and breakage probability developed above are only valid for this subrange. However, as discussed previously, this change is acceptable since the very small eddies have very low energy contents and very short lifetimes thereby having a negligible effect on the breakage of bubbles.

Tennekes and Lumley (1972) have given the minimum size of eddies in the inertia subrange as $2\pi\lambda_d/\lambda_{min} \approx 0.2\text{-}0.55$ or $\lambda_{min}/\lambda_d \approx 11.4\text{-}31.4$.

Substituting Equations (3.16) and (3.27) into Equation (3.28), the breakup rate of bubbles of size v_i or d_i into a size of $v_i f_{BV}$ can be obtained as

$$\Omega_B(v_i : v_i f_{BV}) = c_3(1-\varepsilon_G)n_i\left(\varepsilon/d_i^2\right)^{1/3}\int_{\xi_{min}}^{1}\frac{(1+\xi)^2 e^{-\chi_c}}{\xi^{11/3}}d\xi \qquad (3.29)$$

where $\xi_{min} = \lambda_{min}/d_i$

The integrand in Equation (3.29) can be expressed by the incomplete gamma functions and is then easy to calculate.

Since f_{BV} is a value in the interval (0,1) and independent of the original bubble size, the total breakage rate of bubbles of size v_i or d_i can be obtained by integrating the above equation in this interval. Hence, the total breakage rate of bubbles of size v_i or d_i is expressed as

$$\Omega_B(v_i) = \frac{1}{2}\int_0^1 \Omega_B(v_i : v_i f_{BV})\, df_{BV} \qquad (3.30)$$

where 1/2 is used to consider that the effective range of f_{BV} is either 0-0.5 or 0.5-1 (the integrand is symmetrical with $f_{BV} = 0.5$).

3.3.4 Breakage kernel or breakage size distribution

The breakage kernel, $\eta(v_i:v_j)$, was first introduced by Valentas *et al.* (1966) to describe the size distribution of daughter drops or bubbles. It was also called a "breakage size function" (Hesketh *et al.*, 1991b) or a "daughter droplet distribution" (Nambiar *et al.*, 1992). For a continuous breakage kernel, $\eta(v_i:v_j)dv_j$ represents the fraction of bubbles of size v_i that break into bubbles of a size between v_j and v_j+dv_j.

However, as mentioned before, the breakage kernel has usually been more or less arbitrarily chosen by previous authors. For binary breakage, Valentas *et al.* (1966) assumed a delta function as the discrete breakage kernel and a truncated normal density function as the continuous breakage kernel. The truncated normal function was also used by other authors such as Coulaloglou and Tavlarides (1977), Chatzi *et al.* (1989) and Chatzi and Kiparissides (1992). However, Narsimhan *et al.* (1979) and Randolph (1969) assumed that a uniform distribution could be used, while Lee *et al.* (1987b) used a beta distribution function. All the functions mentioned above, except the uniform distribution, have the same characteristics; a decreasing breakage percentage appears when $v_l \rightarrow 0$ or v_i, while the equal sized breakage has the highest probability.

As pointed out by Nambiar *et al.* (1992), the models that have hitherto assumed a uniform or a truncated normal function-like distribution, centered at $v_i/2$ for the daughter bubble or drop size, may not be representative of the underlying physical situation. The physical situation is clear; more energy is required for binary equal sized breakage than binary unequal sized breakage. This physical concept is also supported by the experimental results of Hesketh *et al.* (1991a) for bubble and drop breakage in turbulent flow. These results show that equal sized breakage has the lowest breakage probability while the highest breakage likelihood occurs when $v_l \rightarrow 0$ (or v_i).

Hence, Hesketh *et al.* (1991b) proposed a so-called $1/X$-shaped kernel function with an adjustable parameter determined by a best fit to their experimental data. However, the $1/X$-shaped function has a zero probability for equal sized breakage, which is in contradiction with their own experimental results. Recently Nambiar *et al.* (1992) proposed a method to predict the breakage kernel for drop breakage in turbulent stirred dispersions based on an eddy interaction model, but this method still predicts a zero possibility for equal sized breakage.

Unlike previous work, the present model does not need any prior assumption as to the distribution function for the breakage kernel. It can be calculated directly from the developed rate function, $\Omega_B(v_i{:}v_i f_{BV})$, describing the rate at which bubbles of size v_i or d_i break into a size of $v_l = v_i f_{BV}$. Together with the total breakup rate of bubbles of size v_i or d_i, $\Omega_B(v_i)$, this gives

$$\eta(v_i : v_j) = \frac{2\int_{\xi_{min}}^{1}(1+\xi)^2\xi^{-11/3}e^{-\chi_c}d\xi}{v_i\int_0^1\int_{\xi_{min}}^{1}(1+\xi)^2\xi^{-11/3}e^{-\chi_c}d\xi df_{BV}} \tag{3.31}$$

3.4 Results and Discussion

3.4.1 Coalescence efficiency

An illustration of the influence of bubble size and energy dissipation rate per unit mass on the bubble coalescence efficiency, using the air-water system as an example, is shown in Figure 3.1 and Figure 3.2.

As can be seen from Figure 3.1, for collisions between bubbles d_i and d_j, the coalescence efficiency generally decreases with an increase in bubble sizes. For a given bubble size d_i, and with a very small d_j, less than about 0.5 mm for instance, the efficiency is very high. However, it decreases very fast with increasing d_j. This is because the coalescence time, as expressed by Equation (3.7), increases much faster than the increase in the interaction time, as expressed by Equation (3.8), when one of the two colliding bubbles is very small. When the value of d_j is close to that of d_i, the coalescence and interaction times reach a similar rate of increase and the coalescence efficiency remains nearly constant. Above this range, with d_j becoming larger and larger, the interaction time will approach a constant value for a given d_i, which can be found from Equation (3.8). However, the coalescence time still increases, and the coalescence efficiency will decrease again.

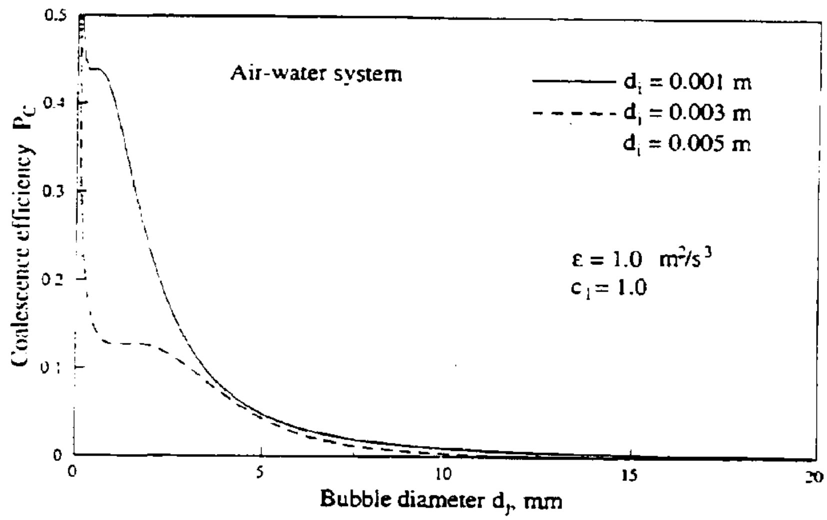

Figure 3.1 Effect of bubble size on the bubble coalescence efficiency in the air-water system.

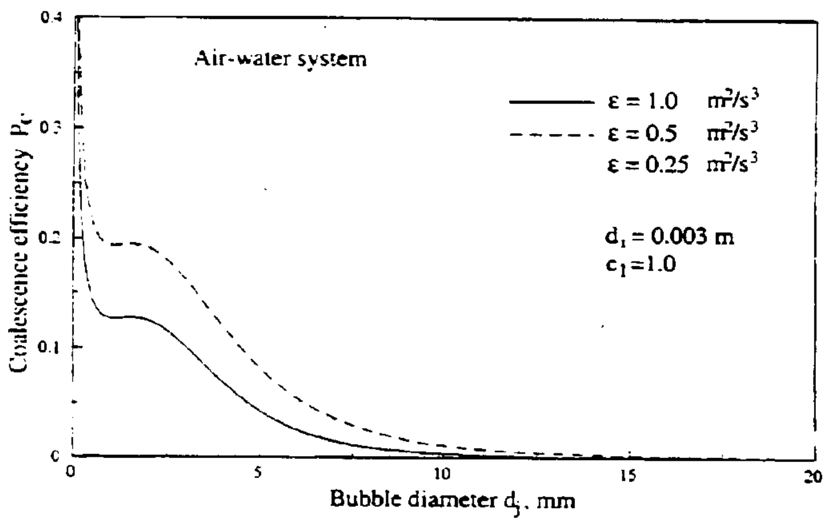

Figure 3.2 Effect of the energy dissipation rate per unit mass on the bubble coalescence efficiency in the air water system.

Figure 3.2 shows the variation in coalescence efficiency with d_j when $d_i = 3$ mm, and with the energy dissipation rate per unit mass, ε, as a parameter. An increase in the energy dissipation rate causes the coalescence efficiency to decrease. The reasons are that the approach velocity of two bubbles in turbulence increases with the energy dissipation rate, and that the coalescence time increases with it. The interaction time is nearly independent of the approach velocity (see Chapter 4).

The effect of other factors such as the physical properties and the constant, c_1, on the bubble coalescence efficiency is not shown in the figures, but can be seen directly from Equation (3.9). It shows that the efficiency decreases with the Weber number. Hence, any increase in liquid density or decrease in surface tension will reduce the efficiency. The value of the constant, c_1, has a similar effect as that of the Weber number. An increase in the density ratio, ρ_G/ρ_L or the virtual mass coefficient, γ, will cause the bubble coalescence efficiency to increase.

3.4.2 Specific coalescence rate

Figure 3.3 and Figure 3.4 show the effects of bubble size and c_1 on the specific bubble coalescence rate, $\Omega_C/(n_i n_j)$, which is the coalescence rate divided by the product of number densities of bubbles i and j. For each given value of d_i, three regions can be identified for the change in the specific coalescence rate with d_j. When d_j is very small, the bubble collision frequency, ω_C, increases with d_j, but the coalescence efficiency, P_C, decreases rapidly, as discussed before. This results in a rapid decrease in the specific coalescence rate, $\Omega_C/(n_i n_j)$, in this region. However, the smaller the value of d_i, the narrower this region. For small values of d_i, *e.g.* $d_i \leq 1$ mm, the region may be disregarded. Above this region, the coalescence efficiency decreases more slowly or is even approximately constant. Then the increase in collision frequency becomes important, and makes the specific coalescence rate increase until a maximum is reached. Above this region, the specific coalescence rate decreases again due to the dominating decrease in the coalescence efficiency. At $c_1 = 1$, the maxima in the specific coalescence rate are located approximately at $d_j = d_i$ for the large bubble sizes. For d_i = 1 mm, the highest specific coalescence rate is found at d_j = 2.5 mm. The result that small bubbles or drops coalesce more rapidly with large particles is a well known fact in water/oil separations.

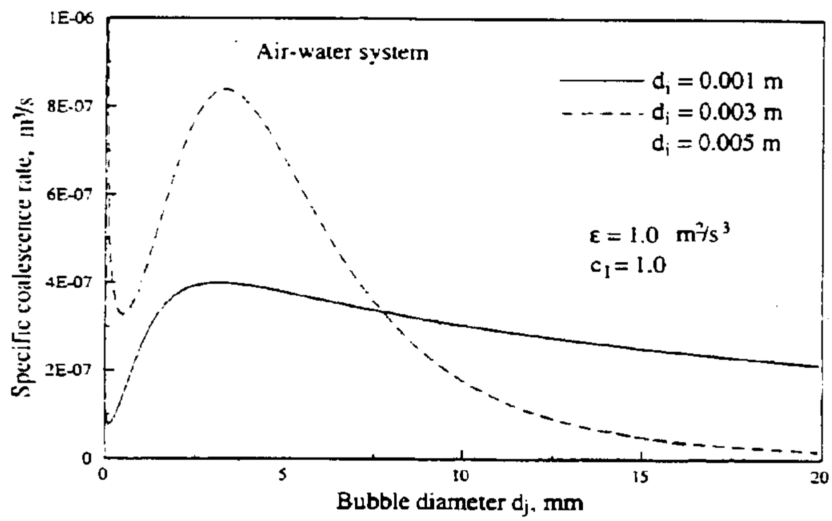

Figure 3.3 Effect of bubble size on the specific bubble coalescence rate, $\Omega_C/(n_i n_j)$, in the air-water system as c_1 = 1.0.

As can be seen by comparing Figure 3.3 and Figure 3.4, the specific coalescence rate is very sensitive to the value of c_1, and the dependency on bubble size also changes.

In general, the change in the specific coalescence rate with the bubble size as predicted by the present model, differs from the results of Lee *et al.* (1987). In their model, the specific coalescence rate increased monotonously with d_j after the initial minimum was reached.

The effect of the energy dissipation rate on the specific coalescence rate is shown in Figure 3.5 and Figure 3.6. The larger the energy dissipation rate, the lower the specific coalescence rate. This shows that the coalescence efficiency is the more sensitive to changes in the energy dissipation rate as it decreases with increasing dissipation rate, whereas the collision frequency increases. For the air-water system and small bubble sizes (d_i = 1 mm), the smaller energy dissipation rates may make the change in the specific coalescence rate with d_j monotonous even for c_1 = 1.0.

The effects of physical properties such as liquid density and surface tension on the specific coalescence rate are qualitatively similar to those for the coalescence efficiency, as discussed before.

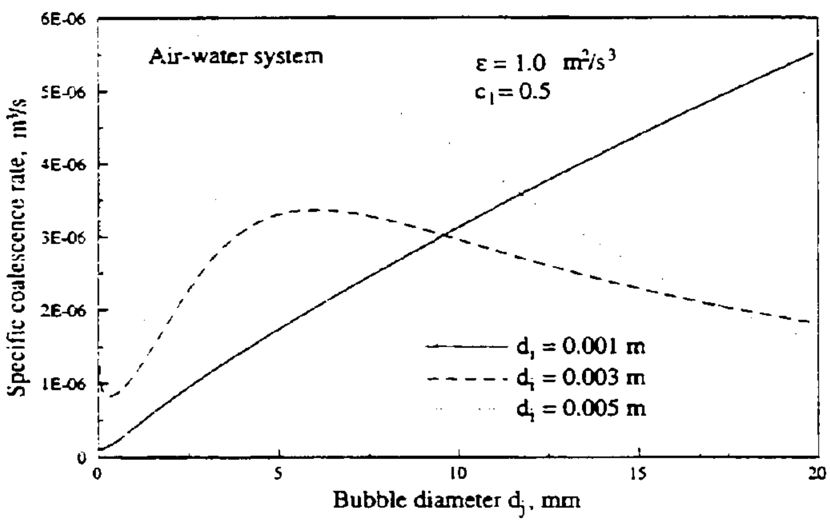

Figure 3.4 Effect of bubble size on the specific bubble coalescence rate, $\Omega_C/(n_i n_j)$, in the air-water system as c_1 = 0.5.

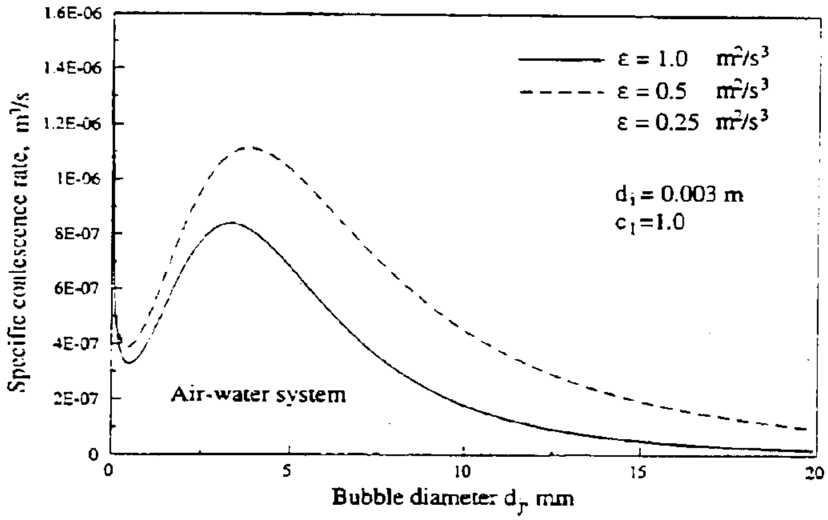

Figure 3.5 Effect of the energy dissipation rate on the specific bubble coalescence rate, $\Omega_C/(n_i n_j)$, in the air-water system.

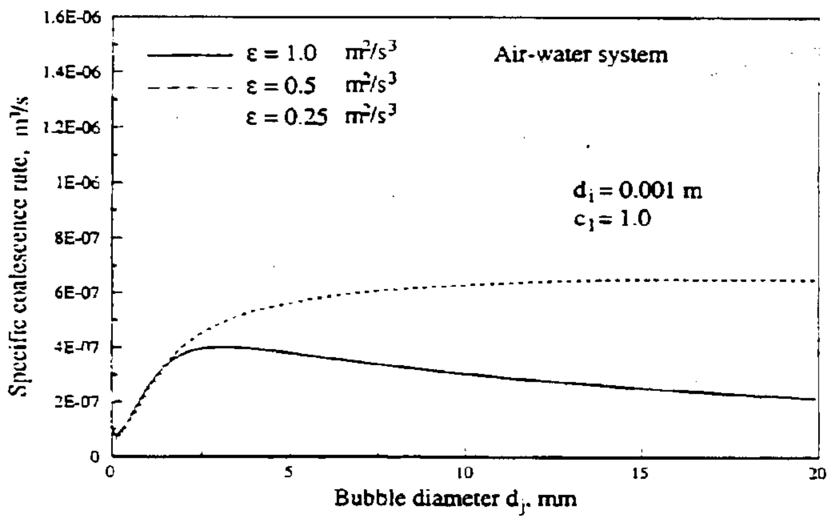

Figure 3.6 Effect of the energy dissipation rate on the specific bubble coalescence rate, $\Omega_C/(n_i n_j)$, in the air-water system.

3.4.3 Breakage kernel

Differing from the previous models for bubble or drop breakage, the present model for bubble breakup rate has no unknown or tuned parameters. The breakage rate and the daughter bubble or drop size distribution can also be predicted, given the operating conditions and the fluid system.

The present model shows that the breakage kernel is usually a function of the original bubble size, the energy dissipation rate and the physical properties. The dimensionless breakage kernel, $\eta\nu_i$, for the air-water system, is illustrated in Figure 3.7. It shows that the dimensionless breakage kernel is a *U*-shaped function and that the lowest possibility is found for equal sized breakage for any given size. This agrees with both physical intuition and the experimental results obtained by Hesketh (1991a,b).

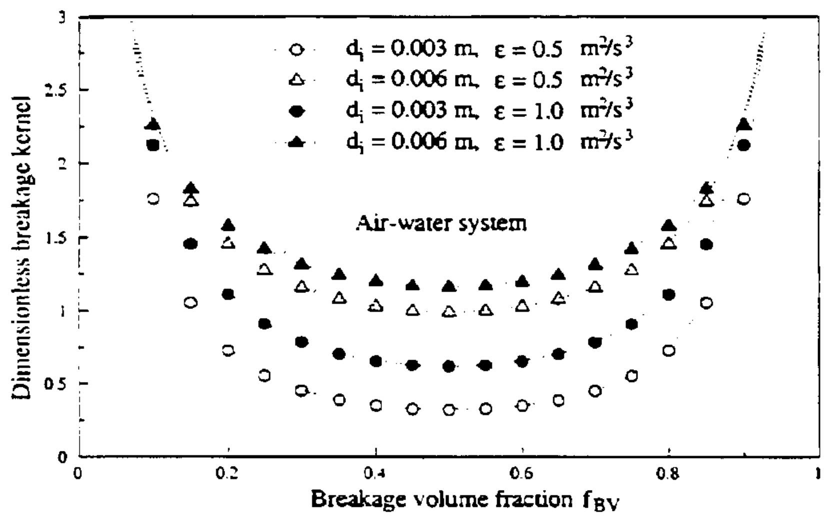

Figure 3.7 Effect of bubble size and energy dissipation rate per unit mass on the dimensionless breakage kernel for the air-water system.

The breakage kernel depends, as mentioned above, not only on the energy dissipation rate, but also on the original bubble size. For larger bubbles, the effect of the energy dissipation rate becomes insignificant and the daughter bubble size distribution tends to become flat. This situation can be seen more clearly in Figure 3.8, where the breakage fraction over every interval 0.05 of f_{BV} is given. This is reasonable, because there is a wider size range of eddies affecting the larger bubbles and then a higher chance for breaking them into daughter bubbles with close to equal sizes. An increase in the energy dissipation rate also makes the distribution flatten since this is equivalent to providing a higher energy for breakage.

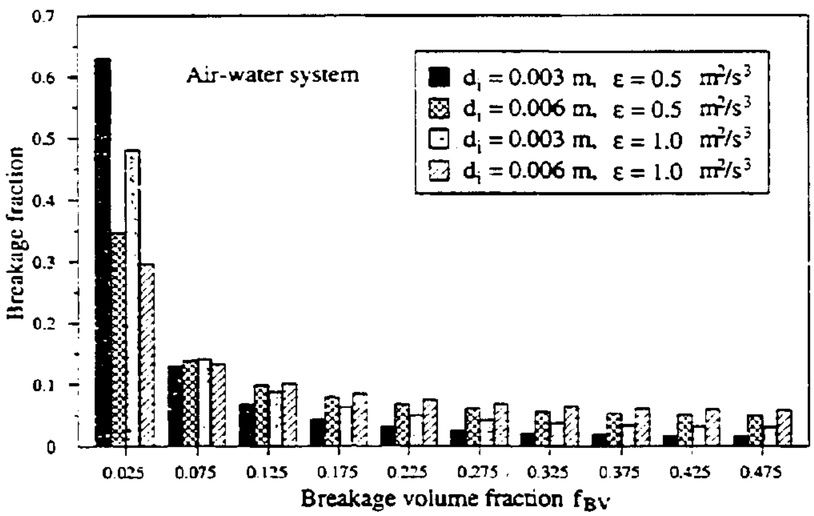

Figure 3.8 Breakage fraction versus the breakage volume fraction with the energy dissipation and bubble size as parameters.

In order to test the bubble breakage model, the predicted breakage fractions for the air-water system in pipeline flows has been compared with the measured results of Hesketh *et al.* (1991a,b), as shown in Figure 3.9. The predicted results by the model of Hesketh *et al.* (1991a,b) are also illustrated in the figure. It can be seen that the agreement between the predicted results of the present model and the experimental results is surprisingly good. In addition, it can be found that, under the high energy dissipation rates, $\varepsilon = 13.3\ m^2/s^3$, prevailing during the experiments, the original bubble size, d_i, has nearly no effect on the daughter bubble distribution or breakage kernel. Furthermore, unlike the models of Hesketh *et al.* (1991b) and Nambiar *et al.* (1992), the present model shows that the fraction of equal sized breakage is not zero, except for very small bubbles or very low energy dissipation rates. This is supported by the experimental results of Hesketh *et al.* (1991a).

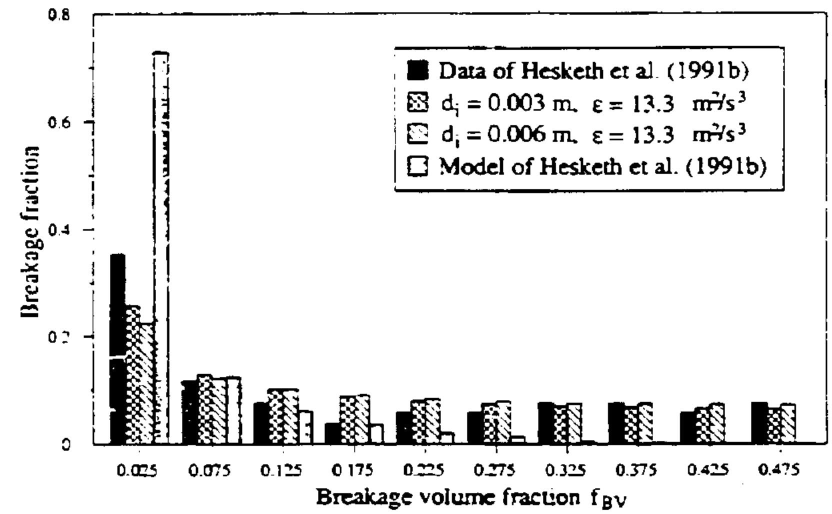

Figure 3.9 Comparison of the predicted breakage fraction by this model with the measured data of Hesketh (1991a).

3.4.4 Specific breakage rate

The influence of bubble size and energy dissipation rate on the specific breakage rate, $\Omega_B/[(1-\varepsilon_G)n_i]$, is shown in Figure 3.10 with the air-water system as an example. The larger the bubble size and/or the energy dissipation rate, the higher the specific breakage rate. This is reasonable since a larger bubble can be hit by a wider range of eddies, and a larger energy dissipation rate means a higher energy content per unit mass of eddies. The specific breakage rate of very small bubbles is close to zero, because the eddies capable of causing the bubbles to oscillate are too small to make them break. As the energy dissipation rate increases, the bubble size, under which no breakage occurs, is decreased.

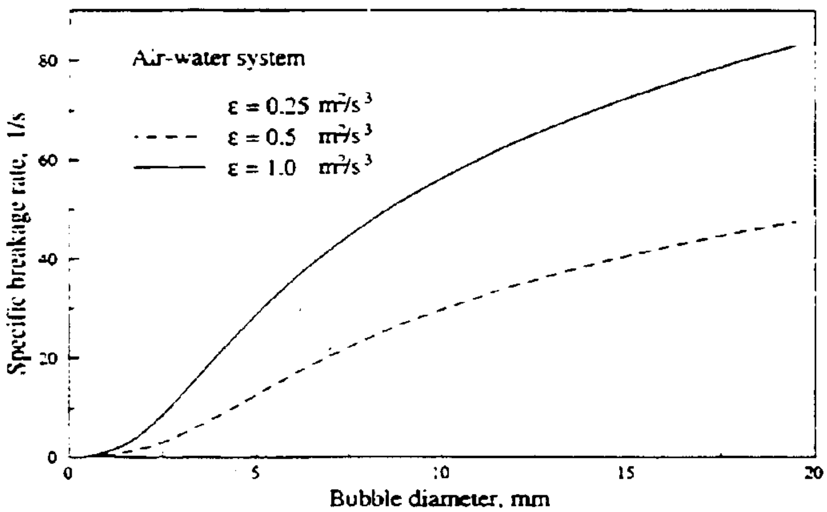

Figure 3.10 Effect of the energy dissipation rate per unit mass on the specific breakage rate, $\Omega_B/[(1-\varepsilon_G)n_i]$, in the air-water system.

3.5 Conclusion

A semi-theoretical turbulent bubble coalescence rate model and a theoretical bubble breakup rate model are developed respectively, based on the principles of molecular collision, probability and turbulence. The bubble coalescence rate model has only one unknown parameter, and the bubble breakage rate model has none unknown parameters and all the constants in the model are determined from the isotropic turbulence theory.

The theoretical bubble breakup rate model has no unknown parameters. The daughter bubble size distribution can directly be derived from the breakage rate model. It has shown very good agreement with the experimental results of Hesketh *et al.* (1991a,b).

The developed models may also be applied to turbulent liquid-liquid dispersions.

However, Equation (3.6), which has been used in describing the coalescence efficiency by many previous investigators and also by this work, is more or less empirical and may be not representative for the real conditions. Besides this, the models of coalescence time and interaction time used in this work also have certain limitations. For instance, Equation (3.7) was developed by Chesters (1991) based on an analysis of equal sized bubble or drop coalescence and assumed the particles having fully mobile interfaces. Equation (3.8) developed in Chapter 4 is based on the parallel film concept which may not be valid for cases when the size difference between two colliding particles is very large. Hence, the coalescence rate model needs further improvement.

A better way of utilizing the t_C and t_I concepts may be to directly apply such a condition for coalescence occurrence as

$$t_I \geq t_C.$$

similar to the modeling method for bubble breakage. More detailed models for t_C are under development (BRIFE/EEC program, Chesters, 1991), also taking mass transfer into account. They may be available at a later stage.

Another way is to simultaneously study each individual bubble collision and liquid film drainage process, instead of obtaining the interaction time and the coalescence time separately as usual.